

알지네이트/수용성 프러시안 블루/환원된 그래핀 옥사이드 복합체를 이용한 전극 개질에 따른 과산화 수소 센서 개발

윤옥자[†] 

중앙대학교 다빈치 교양대학

(2018년 8월 6일 접수, 2018년 9월 13일 수정, 2018년 9월 19일 채택)

A Hydrogen Peroxide Electrochemical Sensor Based on an Alginate/Water-Soluble Prussian Blue/Reduced Graphene Oxide Composite Modified Electrode

Ok Ja Yoon[†] 

Da Vinci College of General Education, Chung-Ang University, Seoul 09974, Korea

(Received August 6, 2018; Revised September 13, 2018; Accepted September 19, 2018)

초록: 다양한 바이오 응용에서 중요한 측정 인자인 과산화 수소(H_2O_2) 센서를 개발하기 위하여, 알지네이트(A) 용액에 수용성 프러시안 블루(s-PB), 그리고 환원된 그래핀 옥사이드(rGO)를 분산시켜 전극 소재를 만들었고 탄소 스크린 프린트 전극에 복합 용액을 젤화 과정을 통해 전극에 고정시켰다. 젤화 과정에서 전극 소재에 남아 있는 염을 제거하기 위하여 충분히 수세를 한 후 실온에서 건조하였다. 전극 소재의 특성은 푸리에 변환 적외선 (FTIR), 전계 방출 주사 전자 현미경(FE-SEM)으로 조사하였다. A/s-PB/rGO 전극을 이용한 순환 전류(CV) 측정 결과를 통해 전극으로써 우수한 전기 화학 반응, 안정성, 재현성을 확인하였고, 미분 펄스 볼타 그래프(DPV)으로 측정한 산화 전류는 4 mM(S/N = 3)의 검출 한계와 높은 감도($2.7 \mu A \cdot mM^{-1} \cdot cm^{-2}$)를 나타내었다. 전기화학적 센서 기반의 전극 개발은 의학 및 환경 응용 분야에서 매우 중요하게 활용될 것으로 판단된다.


Abstract: An electrochemical H_2O_2 sensor was developed using an alginate/water-soluble prussian blue/reduced graphene oxide (A/s-PB/rGO) composite on carbon screen printed electrodes for use in bioapplications. Carbon screen-printed working electrodes were modified with A/s-PB, A/rGO, and A/s-PB/rGO composite solutions by *in situ* gelation. The composites were characterized by Fourier transform infrared spectroscopy and field emission scanning electron microscopy. The cyclic voltammetric measurements made using the electrode modified by A/s-PB/rGOs showed improved electrochemical reaction and stability over the A/s-PB and A/rGO modified electrodes. A two-electron transfer process is indicated at the modified electrode surface. The oxidation current showed a detection limit of 4 mM (S/N = 3) and linear range of 4–28 mM. The A/s-PB/rGO modified electrode provides a tool for high-sensitivity ($2.7 \mu A \cdot mM^{-1} \cdot cm^{-2}$) and stable H_2O_2 analyses with a low limit of detection. Development of biosensor-based modified electrodes is important for biomedical and environmental applications.

Keywords: A/s-PB/rGO modified electrode, A/s-PB modified electrode, A/rGO modified electrode, electrochemical sensor, hydrogen peroxide.

Introduction

Hydrogen peroxide (H_2O_2), as a kind of reactive oxygen species, is an important signaling molecule in the biological processes associated with many diseases,¹ as well as in food manufacturing,² pharmaceutical,³ and environmental applica-

tions.⁴ Electrochemical biosensors have been used for medical, biological and biotechnological applications such as real-time electrochemical neurotransmission monitoring, H_2O_2 and cell-based biosensing, and antibody fragments or antigens used to monitor binding.⁵ Development of electrochemical sensors for H_2O_2 detection has focused on the enhanced electrochemical sensitivity of electrodes modified by nanomaterials such as one-dimensional carbon nanotubes (CNTs), two-dimensional graphene, or reduced graphene oxide (rGO) and prussian blue (PB) on bare gold and glassy carbon electrodes.^{6–8} In recent

[†]To whom correspondence should be addressed.
yokk777@cau.ac.kr, 0000-0003-1023-9536
©2018 The Polymer Society of Korea. All rights reserved.

years, electrodes modified using two-dimensional graphene or rGO have also been investigated because of their unique properties such as fast electron transport, good biocompatibility, high thermal conductivity, and electro-activity for redox reactions.⁹ Two-dimensional graphene modified electrodes used as electrochemical sensors have enhanced ability to detect the electrocatalytic activity of small biomolecules such as enzymes, dopamine, H_2O_2 and nicotinamide adenine dinucleotide (NADH).¹⁰ The physical and electrochemical properties of rGO, such as carbon structures, defects, and functional groups on the surface have been used in electrochemical applications.¹¹ Studies have shown electrochemically rGO modified electrodes used for electrochemical sensing of nitric oxide¹² and detection of tyrosine¹³ and H_2O_2 .¹⁴

Researchers have reported high sensitivity and detection limits using electrodes modified by rGO/PB composites for glucose,¹⁵ dopamine, and H_2O_2 sensing,¹⁶ spontaneous deposition of PB on rGO-gold nanoparticle composites,⁷ and other compounds.¹⁷ PB or ferric ferrocyanide ($\text{Fe}_4[\text{Fe}(\text{CN})_6]_3$) has been investigated for use in electrochromic applications,¹⁸ secondary batteries,¹⁹ chemical and biological sensors,²⁰ and hydrogen storage.²¹ The electroactive layers of PB deposited onto the surface of an electrode has been improved by forming composites of PB with different nanomaterials.²⁰ However, PB is insoluble in most common solvents and dispersion of PB into a solvent is needed to make composites with various nanomaterials or polymers. A water-soluble form of PB (s-PB; $\text{C}_6\text{Fe}_2\text{KN}_6 \cdot x\text{H}_2\text{O}$) is known as an inorganic pigment containing ferric ferrocyanide and has been used to track transplanted cells such as mesenchymal stem cells²² and monitor iron oxide particle labeling dilution through cell division.²³ Alginate/CNT composite modified electrodes formed by *in situ* gelation have been used to monitor caffeic acid derivatives. The alginate forms an interconnected CNT network on a modified electrode.²⁴ Sodium alginate (SA) is a natural polysaccharide used for the removal of pollutants from water and is an excellent natural adsorbent.²⁵ SA as immobilized agent was formatted the water-insoluble alginate hydrogel with hydrophobicity by binding of Na^+ ions dissociated from the polysaccharides and divalent cations such as Ca^{2+} .²⁶ The sodium alginate was converted to calcium alginate gel and the alginate composite was obtained by washing. Other researchers have reported that alginate and rGO composites become hydrophilic and the rGO can be well dispersed.²⁵

In this study, we develop A/s-PB/rGO composite modification of a carbon screen printed electrode (SPE) for the elec-

trochemical sensing of H_2O_2 . The A/s-PB/rGO modified electrode is used in cyclic voltammetry (CV) and differential pulse voltammetry (DPV) studies as a H_2O_2 biosensor and its suitability as an electrode material was assessed.

Experimental

Preparation of rGO. GO sheets were synthesized from purified natural graphite flakes (Sigma Aldrich, St. Louis, MO, USA) using a modified Hummers' method.²⁷ For reduction of the GO sheets, a solution of GO sheets (6 mg) and deionized water (2 mL) was dispersed by ultrasonication for 2 h. To this, 15 mL of *N,N'*-dimethylformamide (DMF, 99.5%; Junsei, Tokyo, Japan) solvent and 1 mL of hydrazine hydrate solution (24 ~ 26%, Sigma Aldrich) were added. The resultant solution was stirred for 24 h at 80 °C and then washed with ethanol at room temperature.

Modification of the Carbon Electrode. The electrochemical sensors used were carbon SPEs (DRP-110, Dropsies, Asturias, Spain) and included: a working electrode (radius=0.2 cm, area=0.13 cm²), a carbon counter electrode, and a Ag/AgCl reference electrode structured on a ceramic platform (34 mm × 10 mm × 0.5 mm). It was connected to a mini potentiostat and controlled by software (Dy2100B, Digi-Ivy, USA). All potentials were measured against the Ag/AgCl electrode.

For modification of the electrodes, a solution of A/s-PB/rGO composite was prepared by mixing 2 wt% sodium alginate (Sigma Aldrich, USA) and water-soluble PB (Sigma Aldrich, USA) powders after 2 wt% concentration of the rGO sheets were sonicated in distilled water (DW, 20 mL). To coat the composite films uniformly on the electrode surface, droplets of SA/s-PB/rGO solution were placed on the surface using a 5 μL micropipette (Accumax Tips, India) and air dried at room temperature. To form *in situ* gelation on the modified electrodes, 30 μL of 2 wt% calcium chloride solution in DW was dropped by micropipette for 1 h and the sodium alginate was converted to the calcium alginate gel. The calcium alginate composite on the carbon SPEs were converted to the alginate composite by washing with DW and drying overnight at room temperature.

Evaluation and Calibration of the Modified Electrode. The experiments with the electrochemical sensors were performed with a 30 μL solution of 10 mM $\text{K}_3[\text{Fe}(\text{CN})_6]$ (99%, Sigma Aldrich). Cyclic voltammetry (CV) was conducted for the modified carbon SPEs using a potentiostat electrochemical workstation. The parameters for the CV were as follows: the potential sweep range was from -0.5 to 0.5 V vs. an Ag/AgCl

according to a scan rate. All the experiments were performed under a sealed tip. The sealed tip was constructed by attaching the upper section of a cut-tip (Sorenson, USA) to the ceramic surface of the SPEs using cyanoacrylate glue. The differential pulse voltammetry (DPV) was conducted after adding 4 mM H_2O_2 (34.5%, Sigma Aldrich) to a phosphate buffer solution (pH 7.4) (Gibco, USA) by applying an initial potential of 1 V, and varying the potential from -1 to 1 V, with increments of 0.005 V, a pulse amplitude of 0.05 V, a pulse width of 0.05 s, a sample width of 0.02 s, and a pulse period of 0.2 s. The calibration for molar concentration of H_2O_2 was performed from 4 to 28 mM by adding 4 mM of H_2O_2 solution.

Analytical Methods. The surfaces of the alginate, s-PB powder, rGO sheets, composite materials of A/s-PB, A/rGO, and A/s-PB/rGO were prepared by coating on a silicon wafer and analyzed by Fourier-transform infrared spectroscopy (FT-IR) (Bruker IFS-66/S, Bruker Corporation, Germany). The modified electrode based electrochemical sensor was imaged using a field emission scanning electron microscope (FE-SEM; JSM 890, JEOL Ltd., Japan).

Results and Discussion

Characteristics of the Composite Materials for the Modified Electrode. The s-PB powder and rGO sheets for the modified electrodes dispersed well on the silicon wafer (Figure 1). The s-PB particles in Figure 1(a) and 1(b) are shown before and after dissolution in DW. The particles were smaller than the average value ranging from $43.28 \pm 39.76 \mu\text{m}$ to $80.7 \pm 7.91 \text{ nm}$, and were more uniform after dissolution. The rGO sheets (Figure 1(c)) were typically $\sim 1.5 \text{ nm}$ thick, as reported by Yoon *et al.*²⁷ Figures 1 (d) and 1(e) show the surface images of the electrodes modified with the A/s-PB and A/rGO composite film, respectively. Figure 1(f) shows the surface of the electrode modified by the A/s-PB/rGO composite. All the surface images of the modified electrode demonstrated that the composite films were formed by good dispersion of the s-PB powder and rGO sheets in alginate solution.

Figure 2 shows the FTIR transmittance spectra ($4500\text{--}700 \text{ cm}^{-1}$) of the alginate, s-PB powder, rGO sheets, and the composite materials of A/s-PB, A/rGO and A/s-PB/rGO.

The absorption peaks of the alginate appeared at $3700\text{--}3000 \text{ cm}^{-1}$ (COO-H/O-H stretching vibration), 1594 cm^{-1} (C=C stretching vibration), 1415 cm^{-1} (O-H stretching vibration), and 1024 cm^{-1} (C-O stretching vibration). The absorption peaks of the rGO sheets appeared at 1596 cm^{-1} (C=C stretching vibration),

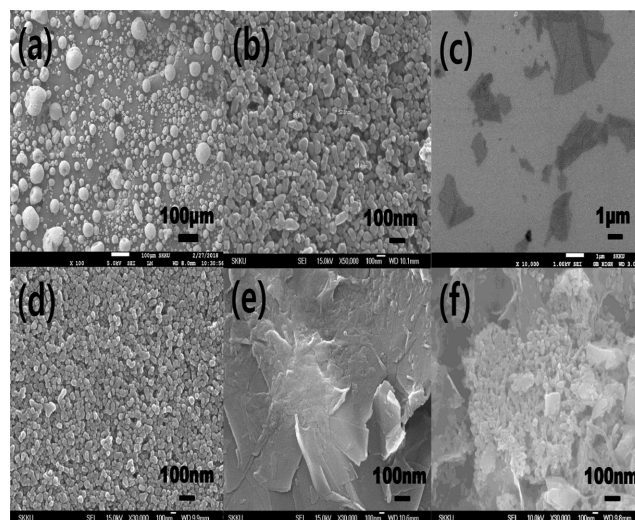


Figure 1. FE-SEM images of (a) the s-PB powders; (b) the s-PB powders after dissolution in DW; (c) rGO sheets, electrodes modified with (d) the A/s-PB composite film; (e) the A/rGO composite film; (f) the A/s-PB/rGO composite film by *in situ* gelation method.

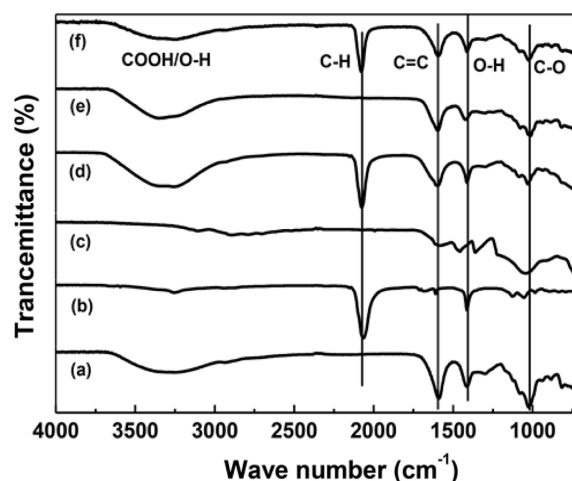


Figure 2. FTIR spectra of (a) alginate; (b) s-PB powder; (c) rGO sheets, and composite materials of (d) A/s-PB; (e) A/rGO; (f) A/s-PB/rGO.

1465 cm^{-1} (O-H stretching vibration), and 1357 and 1047 cm^{-1} (C-O stretching vibration).

The absorption bands of the s-PB powder appeared at 2064 cm^{-1} (C-H stretching vibration), 1610 cm^{-1} (C=C stretching vibration), 1411 cm^{-1} (O-H stretching vibration), and 1126 and 1052 cm^{-1} (C-O stretching vibration). The 2073 cm^{-1} (C-H stretching vibration) peak in the spectra of the A/s-PB composite compared to those of the alginate and s-PB powder indicates characteristics of the s-PB powder. The peak at 3700--

3000 cm^{-1} (COO-H/O-H stretching vibration) in the A/rGO composite spectra compared to those of the alginate and rGO sheets spectra is related to the characteristics of the rGO sheets.²⁸ Spectral analysis demonstrated that the composite materials combined well with dispersion of the s-PB powder and rGO sheets in the alginate solution.

Electrochemical Characterization of the Modified Electrode. The working electrode was a composite film formed from a 5 μL drop of A/s-PB/rGO solution (Figure 1(f)). The composite modified working electrode, carbon counter electrode, and Ag/AgCl reference electrode were measured for CV. The CV curves of the A/s-PB/rGO modified electrode vs. the Ag/AgCl reference electrode at different values of ν (10, 30, 50, 70, and 90 mVs^{-1}) in 10 mM $\text{K}_3[\text{Fe}(\text{CN})_6]$ solution at a volume of 30 μL are shown in Figure 3(a). For sensitivity comparison analysis of the A/s-PB/rGO modified electrodes, CV measurements from the composite modified electrode and carbon SPE were carried out at a scan rate (ν) of 50 mVs^{-1} in the 10 mM $\text{K}_3[\text{Fe}(\text{CN})_6]$ solution (Figure 3 (b)). The peak current of the A/s-PB/rGO modified electrode increased significantly compared to those of the carbon and

other composite modified electrodes.

The difference between the cathodic and anodic potential peaks, $\Delta E_p = |E_{pc} - E_{pa}|$ at $\nu = 50 \text{ mVs}^{-1}$ measured 199 mV. ΔE_p increased linearly with increasing scan rate. The ratio of I_{pa} to I_{pc} is close to one. These results demonstrated that the redox process is an electrochemically quasi-reversible process. The relationships between the anodic (I_{pa}) and cathodic (I_{pc}) peak currents and $\nu^{1/2}$ are shown in Figure 3(c). The linear regression equations are $I_{pa} = 18.67 \nu^{1/2} + 1.62$ (μA , ($\text{mVs}^{-1})^{1/2}$, $R^2 = 0.97$) and $I_{pc} = -17.93 \nu^{1/2} + 1.31$ (μA , ($\text{mVs}^{-1})^{1/2}$, $R^2 = 0.98$). The linear dependence of I_p vs. $\nu^{1/2}$ indicates diffusion controlled redox processes.²⁹

The anodic peak potential (E_{pa}) and the cathodic peak potential (E_{pc}) as a function of the natural logarithm of ν in Figure 3(d), are $E_{pa} = 0.05 \log \nu + 0.007$ (ν , $\log (\text{mVs}^{-1})$, $R^2 = 0.93$) and $E_{pc} = -0.065 \log \nu + 0.006$ (ν , $\log (\text{mVs}^{-1})$, $R^2 = 0.97$), respectively. From Laviron's equation,³⁰ the slopes of I_{pa} and I_{pc} in Figure 3(c) correspond to $2.3 RT/(1-\alpha) nF$ and $-2.3 RT/\alpha nF$, respectively, where $R = 8.314 \text{ J mol}^{-1} \text{ K}^{-1}$, $T = 298 \text{ K}$, $F = 96493 \text{ C mol}^{-1}$, α is the electron transfer coefficient, and n is the electron transfer number.

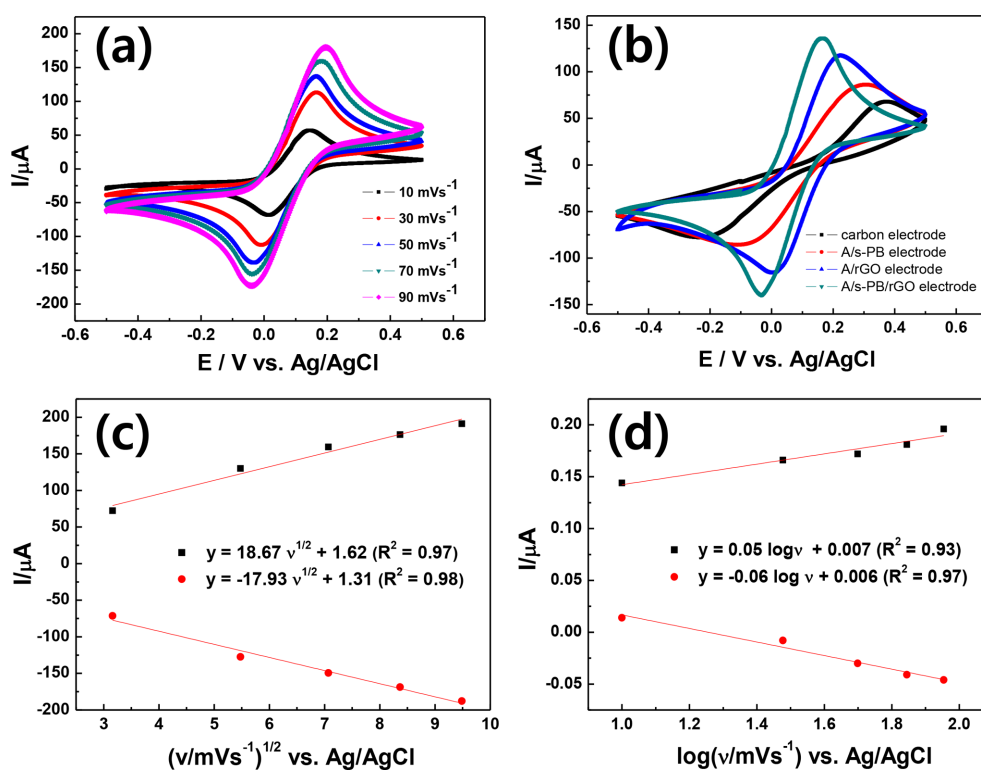


Figure 3. (a) The CV curves of the composite modified carbon SPEs vs. Ag/AgCl at potential sweep rates of 10, 30, 50, 70, and 90 mVs^{-1} in 10 mM $\text{K}_3[\text{Fe}(\text{CN})_6]$; (b) CV curves of the A/s-PB/rGO modified, A/rGO modified, A/s-PB modified and bare carbon SPE; (c) relationships between $\nu^{1/2}$ and the peak currents I_{pa} and I_{pc} ; (d) the linear regression equations of E_{pa} and E_{pc} vs. the natural logarithm of ν .

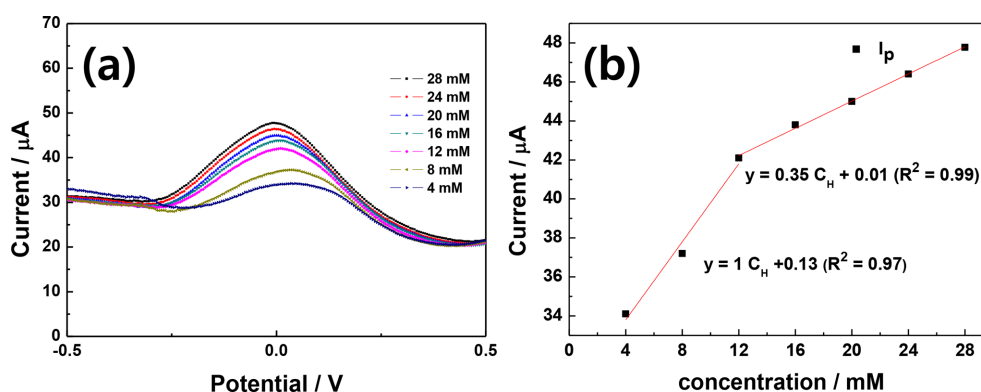


Figure 4. (a) DPV of different concentrations of H₂O₂ (4, 8, 12, 16, 20, 24, and 28 mM); (b) Calibration plot of I_p vs. C_H plot at various H₂O₂ concentrations.

The α and n values were proved to be 0.48 and 1.9, respectively. The redox reaction at the A/s-PB/rGO modified electrode was a two-electron oxidation process.³¹

Calibration of the H₂O₂ Concentration on the A/s-PB/rGO Modified Electrode. For the electrochemical sensing of H₂O₂ for bioapplications, DPV curves were used to obtain a calibration plot for oxidation peak current increasing from 4 to 28 mM in a pH 7.4 phosphate buffer solution. The linear function of the calibration plot (Figure 4(a)) shows two different slopes corresponding to the H₂O₂ concentration ranges of 4–12 and 12–28 mM. The calibration of I_{pa} was calculated as the linear function of $I_p = 0.35C_H + 0.01$ (μA , $R^2 = 0.99$) and $I_p = 1C_H + 0.13$ (μA , $R^2 = 0.97$) in the ranges of 4–12 and 12–28 mM, respectively (Figure 4(b)). Electrochemical sensing using the A/s-PB/rGO modified electrode showed good linearity, a detection limit of 4 mM, a wide dynamic range (4–28 mM for H₂O₂ concentration) and high sensitivity ($2.7 \mu A \text{ mM}^{-1} \text{ cm}^{-2}$). The performance of the A/s-PB/rGO modified electrode was better than the SPEs modified with PB nanoparticles by piezoelectric inkjet printing (sensitivity = $762 \mu A \text{ mM}^{-1} \text{ cm}^{-2}$ and detection limit of $2 \times 10^{-7} \text{ M}$).³² Yoon *et al.* showed that an indium tin oxide electrode modified with graphene and Nafion composite had a H₂O₂ detection limit of 1 mM and sensitivity of $82.6 \mu A \text{ mM}^{-1} \text{ cm}^{-2}$.²⁷

Stability of the Modified Electrode. The stability of the A/s-PB/rGO modified electrode was also measured by repetitive potential sweeps at a scan rate of 50 mVs^{-1} in 10 mM K₃[Fe(CN)₆] solution. The peak current showed only a minor shift after 20 repetitive scans. The CV response of the A/s-PB/rGO modified electrode after 24 h showed no changes compared to the initial signal in Figure 5. The results confirmed the long-term stability of the A/s-PB/rGO modified electrode.

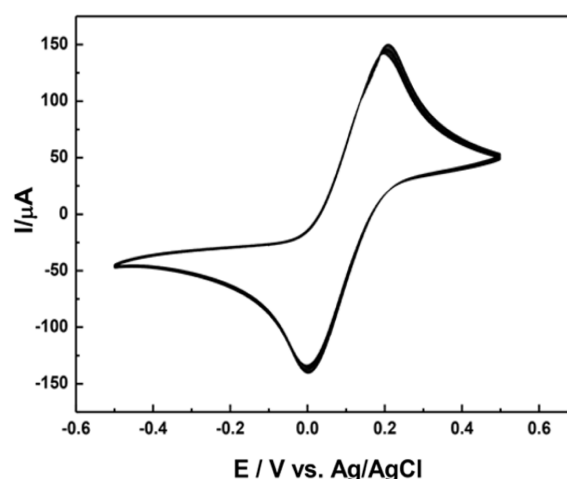


Figure 5. Twenty times CV curves of the A/s-PB/rGO modified electrode vs. Ag/AgCl with potential sweep rates of 50 mV s^{-1} in 10 mM K₃[Fe(CN)₆].

Conclusions

A new composite modified electrode for the detection of H₂O₂ was developed using carbon SPEs modified with A/s-PB/rGO composite film applied by *in situ* gelation. The A/s-PB/rGO modified electrodes showed excellent electrochemical sensing characteristics with good sensitivity, linear response, and stability. The CV measurements using the A/s-PB/rGO modified electrode showed better and more stable oxidation reaction compared to the electrochemical signals obtained by the A/s-PB and A/rGO modified electrodes. The DPV measurements showed high sensitivity ($2.7 \mu A \text{ mM}^{-1} \text{ cm}^{-2}$), the detection limit of 4 mM ($S/N = 3$), and a linear range of 4 to 28 mM. The results of the A/s-PB/rGO modified electrode

indicate that this electrode can provide enhanced detection of H_2O_2 in bioapplications.

Acknowledgements: This research was supported by the Basic Science Research Program through the National Research Foundation of Korea (NRF) under the auspices of the Ministry of Education (Grant No. 2009-0093817, 2015R1C1A2A 01056280 and 2018R1D1A1B07050778).

References

1. E. A. Veal, A. M. Day, and B. A. Morgan, *Mol. Cell*, **26**, 1 (2007).
2. B. Zhang, Y. Cui, H. Chen, B. Liu, G. Chen, and D. Tang, *Electroanalysis*, **23**, 1821 (2011).
3. V. Aroutiounian, V. Arakelyan, M. Aleksanyan, A. Sayunts, G. Shanhazaryan, P. Kcer, P. Picha, J. Kovarik, J. Pekarek, and B. Joost, *Sensors & Transducers*, **213**, 46 (2017).
4. A. Asghar, A. A. A. Raman, and W. M. A. W. Daud, *J. Clean. Prod.*, **87**, 826 (2015).
5. D. Grieshaber, R. MacKenzie, J. Vörös, and E. Reimhult, *Sensors*, **8**, 1400 (2008).
6. A. M. Farah, N. D. Shooto, F. T. Thema, J. S. Modise, and E. D. Dikio, *Int. J. Electrochem. Sci.*, **7**, 4302 (2012).
7. X. Bai and K.-K. Shiu, *Electroanalysis*, **27**, 74 (2015).
8. D. Moscone, D. D'Ottavi, D. Compagnone, and G. Palleschi, *Anal. Chem.*, **73**, 2529 (2001).
9. T. Kuila, S. Bose, P. Khanra, A. K. Mishra, N. H. Kim, and J. H. Lee, *Biosens. Bioelectron.*, **26**, 4637 (2011).
10. Y. Shao, J. Wang, H. Wu, J. Liu, I. A. Aksay, and Y. Lina, *Electroanalysis*, **22**, 1027 (2010).
11. M. Wei, L. Qiao, H. Zhang, S. Karakalos, K. Ma, Z. Fu, M. T. Swihart, and G. Wu, *Electrochim. Acta*, **258**, 735 (2017).
12. J. Wei, J. Qiu, L. Li, L. Ren, X. Zhang, J. Chaudhuri, and S. Wang, *Nanotechnology*, **23**, 335707 (2012).
13. Y.-L. Wang and G.-C. Zhao, *Int. J. Electrochem.*, **6**, 2011 (2011).
14. L. Cao, Y. Liu, B. Zhang, and L. Lu, *ACS Appl. Mater. Interfaces*, **2**, 2339 (2010).
15. X. Bai, G. Chen, and K.-K. Shiu, *Electrochim. Acta*, **89**, 454 (2013).
16. J. Li, Y. Jiang, Y. Zhai, H. Liu, and L. Li, *Anal. Lett.*, **48**, 2786 (2015).
17. M. Zhou, Y. M. Zhai, and S. J. Dong, *Anal. Chem.*, **81**, 5603 (2009).
18. J. Velevska, M. Pecovska-Gjorgjevich, N. Stojanov, and M. Najdoski, *IJSBAR*, **25**, 380 (2016).
19. Z. Liu, G. Pulletikurthi, and F. Endres, *ACS Appl. Mater. Interfaces*, **8**, 12158 (2016).
20. A. A. Karyakin, *Electroanalysis*, **13**, 813 (2001).
21. C. P. Krap, J. Balmaseda, B. Zamora, and E. Reguera, *Int. J. Hydrogen Energy*, **35**, 10381 (2010).
22. G. Schmidtke-Schrezenmeier, M. Urban, A. Musyanovych, V. Miländer, M. Rojewski, N. Fekete, C. Menard, E. Deak, K. Tarte, V. Rasche, K. Landfester, and H. Schrezenmeier, *Cytotherapy*, **13**, 962 (2011).
23. D. Liu, C. Chen, G. Hu, Q. Mei, H. Qiu, G. Long, and G. Hu, *Acta Biochim. Biophys. Sin.*, **43**, 301 (2011).
24. B. Wei, J. Wang, Z. Chen, and G. Chen, *Chem. Eur. J.*, **14**, 9779 (2008).
25. J. Feng, H. Ding, G. Yang, R. Wang, S. Li, J. Liao, Z. Li, and D. Che, *J. Colloid Interface Sci.*, **508**, 387 (2017).
26. H. Basu, S. Saha, M. V. Pimple, and R. K. Singh, *J. Environ. Chem. Eng.*, **6**, 4399 (2018).
27. O. J. Yoon, C. Y. Jung, I. Y. Sohn, H. J. Kim, B. Hong, M. S. Jhon, and N.-E. Lee, *Compos. Part A*, **42**, 1978 (2011).
28. O. J. Yoon, C. H. Kim, I. Y. Sohn, and N.-E. Lee, *Sensor. Actuat. B*, **88**, 454 (2013).
29. M. Mazloum-Ardakani, H. Rajabi, and H. Bietollahi, *J. Argent. Chem. Soc.*, **97**, 106 (2009).
30. E. Laviron, *J. Electroanal. Chem.*, **101**, 19 (1979).
31. M. Xi, Y. Duan, X. Li, L. Qu, W.L. Sun, and K. Jiao, *Microchim. Acta*, **170**, 53 (2010).
32. S. Cinti, F. Arduini, D. Moscone, G. Palleschi, and A. J. Killard, *Sensors*, **14**, 14222 (2014).